Received: 26 December 2020 | Revised: 13 May 2021 | Accepted: 20 June 2021

IET Renewable Power Generation

DOI: 10.1049/rpg2.12248

The Institution of Engineering and Technology WILEY

ORIGINAL RESEARCH PAPER

Optimal power regulation for wind integration in the balancing market environment

Xue Lyu[1] | Dominic Groß[2] | Zhao Xu[3] | Zhaoyang Dong[4] | Youwei Jia[1]

[1] Department of Electrical and Electronic Engineering, Southern University of Science and Technology, Shenzhen, China

[2] Department of Electrical and Computer Engineering, University of Wisconsin Madison, Madison, Wisconsin, USA

[3] Department of Electrical Engineering, The Hong Kong Polytechnic University, Hong Kong, China

[4] School of Electrical Engineering and Telecommunications, The University of New South Wales, Sydney, Australia

Correspondence
Youwei Jia, Room 543, Engineering building south tower, Southern University of Science and Technology, Shenzhen 518055, China.
Email: jiayw@sustech.edu.cn

Funding information
Natural Science Foundation of China, Grant/Award Number: 72071100; Guangdong Basic and Applied Basic Research Fund, Grant/Award Number: 2019A1515111173; Young Talent Program of Guangdong, Grant/Award Number: 2018KQNCX223; High-level University Fund, Grant/Award Number: G02236002

Abstract

Variable renewable generation and load fluctuations induce significant balancing cost in power system operation. To overcome this issue, this paper proposes a control architecture that leverages inherent regulation capabilities of wind turbines to minimize the system-wide balancing costs. Instead of handling wind power fluctuations via power filtering algorithms that are agnostic to system-wide power imbalance, this paper aims to optimize the wind power generation profile from system perspective. In the proposed method, wind turbines are modelled as semi-dispatchable units, where the dispatch command is dynamically generated at every automatic generation control cycle by considering mileage payments as an indicator of system-wide imbalance. As a result, local resources of wind turbines are optimally leveraged in real-time to mitigate system-wide power imbalances. The proposed strategy and state-of-the-art techniques are compared in comprehensive high-fidelity case studies. Our simulation results demonstrate that the proposed system-aware regulation scheme can alleviate system balancing costs without investments into energy storage systems.

1 | INTRODUCTION

In recent years wind power generation has seen a dramatic increase in the energy mix of modern power systems. Although wind energy is a sustainable and abundant resource, its weather-dependent nature leads to uncertain and intermittent power generation. Conventionally, wind turbines (WTs) operate in a "free-running" manner using maximum power point tracking (MPPT) control. In this operating mode, fast wind power fluctuations will directly result in a fluctuating power imbalance in the power grid and the control of conventional generators (i.e. inertia response, primary control, secondary control, and tertiary control) will respond to the above-mentioned power imbalance [1]. Consequently, the system balancing cost will increase. According to a real-world study in the United Kingdom, the additional balancing costs incurred as the result of 20% integration of wind power would be £200 million per year or £3/MWh [2]. Currently, some market policies have been set up to impose penalties on wind farms (WFs) such as fixed balancing fees per MWh or MW-month [3], and penalties for diverging from the day-ahead forecast [4]. In United Kingdom, wind farms and large loads are allocated a share of the hourly balancing cost that is proportional to their power generation [5]. Because power imbalances are created jointly by demand fluctuations, wind power, and other renewable resources, precisely determining the balancing cost incurred by WFs is a highly complex problem that is not fully addressed by fixed balancing fee schemes currently used by system operators. Moreover, due to limited forecasting accuracy, imposing penalties on deviations from the day-ahead forecast may encourage

WFs to follow the day-ahead forecasts and underutilize wind generation.

An essential ancillary service is automatic generation control (AGC) (i.e. secondary control), which aims to compensate the mismatch between power generation and demand on the time scale of seconds. One widely used metric to quantify the AGC balancing cost are so called mileage payments to AGC units that have seen wide spread adoption (see e.g. FERC order 755 [6]). The regulation mileage reflects the performance of AGC units, and encourages fast-responding AGC units to provide regulation service [7]. In this scenario, the stochastic characteristic of wind power will result in significant mileage payments. To address this problem, a cooperative scheme is proposed in [8] to exploit the complementary characteristics of wind power and battery storage by designing an optimal bidding strategy in joint energy and regulation markets. A combined heat and power plant and a wind farm are operated as a portfolio in [9] to increase the overall profit in a balancing market. It should be noted that, in these works, the fluctuation of wind power is compensated by other flexible resources and not by the WTs themselves. Moreover, existing works focus on determining optimal bidding strategies for relatively long energy scheduling cycles and ignore detailed WTs models, their practical operation constraints, and WT real-time control and operation.

At the real-time control level, wind power fluctuations are normally compensated through smoothing control strategies, where the smoothing references are typically generated through ad-hoc strategies. For example, a first order low pass filter (LPF) is utilized in [10] to smooth out high-frequency components of wind power generation. The control performance of such algorithms greatly depends on choosing an appropriate filtering time constant. Likewise, a wavelet-enabled approach is utilized in [11, 12] for wind power smoothing. A moving average (MA) algorithm is adopted in [13, 14] to eliminate short-cycle power fluctuations and the resulting smoothing effect depends on the filter window size. In addition, the output of a WT is adjusted by pre-setting ramp limits at different time scales in [15, 16]. It should be noted that smoothing references generated by ad-hoc methods do not account for system-wide power imbalance and the resulting smooth generation profiles may be (i) economically inefficient because a significant amount of wind energy may be arbitrarily sacrificed through the predefined hard-coded smoothing algorithms and (ii) not conducive to the reduction of balancing cost because it does not account for system-wide imbalances [17].

In the literature, two broad classes of methods for compensating wind power fluctuations and tracking dispatch commands have been proposed: (i) integration with energy storage systems (EES), and (ii) ESS-free control methods. The first class of methods utilizes ESS to store/release excess energy as needed to obtain a wind energy system that is dispatchable and able to assist in generation-demand balancing [18–20]. While this approach is highly effective, it is also costly due to the significant costs of an ESS. The second class of methods aims to fully leverage the regulation capabilities of WTs without relying on an ESS. Even though the regulation capability of WTs is limited, appropriate control methods can operate WTs as "semi-dispatchable"

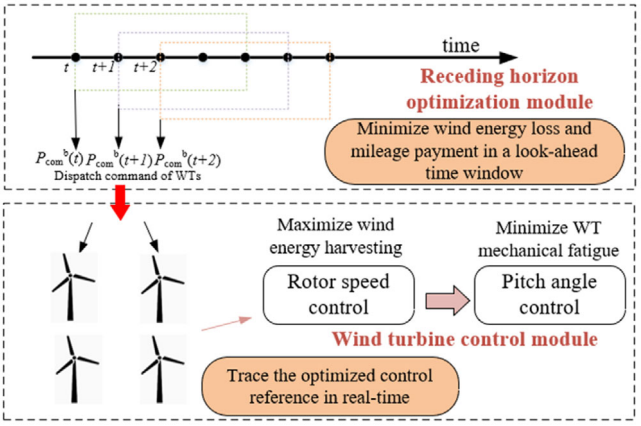

FIGURE 1 Proposed system-perceived wind power regulation framework

units that partially contribute to mitigating system-wide imbalances. Considering the increasing integration of wind generation in large-scale systems, the ESS-free control method is a promising cost-effective solution. Therefore, this work focuses on how to optimally leverage the self-regulation potential of WTs on the time scales of AGC. One potential approach is to curtail wind power generation by adjusting the blade pitch angle [21, 22]. However, relying purely on blade pitch angle control is not economical because the curtailed power is discarded. In addition, frequent changes in the pitch angle will inevitably increase WT mechanical stress and fatigue. Another option is to use the kinetic energy (KE) stored in the WT rotor [23–25] to compensate power fluctuations. This approach is advantageous for energy harvesting because some of the curtailed power can be stored by the WT in the form of KE. This KE can be rapidly released into the grid if increased power injection is requested. Even though utilizing the existing degrees of freedom of WTs to regulate wind power is a promising solution to mitigating system-wide imbalances, it is difficult to quantify and leverage the regulation capabilities of WTs in real-time operation.

To overcome these limitations, a novel wind power regulation paradigm is proposed in this paper. Instead of acting as power sources using MPPT control, we use mileage costs as a metric for system-wide imbalance and regulate wind power generation in real-time. In contrast to existing works, the power reference generated by the proposed method accounts for the overall system imbalance and fully leverages the downward/upward power regulation potential of WTs. The overall architecture is illustrated in Figure 1.

Specifically, at the upper level, we assume that the relevant information, e.g. the power/energy scheduling profile and regulation capacity, mileage cost, and performance scores of AGC units are provided by the system operator. Based on this information the wind farm operator solves a receding horizon optimization problem that trades off maximizing wind power production and minimizing the system-wide balancing cost. At the WT level, a prioritized control strategy is devised to enable WTs to instantly track the dispatch commands received from the upper layer. This architecture is motivated by current market paradigms in different system (i.e. UK national grid, PJM, and

China Southern Power Grid) and wind farm control architectures.

Overall, the contributions of this paper are twofold:

1. We propose a new real-time wind power regulation paradigm that uses mileage costs as a key metric for controlling WTs active power injection.
2. The proposed control framework fully leverages the WTs upward/downward power regulation capabilities to respond to system balancing needs while accounting for WTs operation constraints, i.e., ensuring the practical feasibility of the proposed control.

2 | SYSTEM-PERCEIVED WIND POWER REGULATION

In this section, we will first review basic principles of system balancing services, mileage payments, and wind power regulation. Subsequently, we will introduce a novel receding horizon wind power control algorithm that accounts for the system balancing needs.

2.1 | A prospective role of wind turbines in balancing market

As discussed in Section 1, the uncertain nature of wind power generation and demand can result in significant balancing costs. At the same time, WTs have some flexibility to regulate their power output downward/upward. As a result, WTs can partially contribute to reducing system-wide power imbalances and balancing cost. This, in turn, can potentially reduce the balancing fees charged to a wind farm or result in additional revenue for the WF operator through novel ancillary services. The focus of this work is to develop a technical solution that allows WFs to leverage their control capabilities to partially contribute to mitigating system-wide power imbalances.

We emphasize that, in real-time operation, it is difficult to accurately quantify the amount of balancing cost caused by a particular WF or load. Consequently, system operators currently use different ad-hoc market policies to impose penalties or balancing costs on wind farms ranging from fixed fees per MWh and month [3] to allocating hourly balancing costs to generators and large-scale loads [5] proportionally to their power generation or demand.

In this context, it appears reasonable for a wind farm to contribute to reducing the balancing cost both to improve system performance and to reduce its own cost for balancing services. To this end, we utilize the mileage payment as an indicator to regulate wind power output. We emphasize that WFs should receive further renumeration for partially contributing to balancing the overall system. However, it is unclear how to accurately price such a service and allocate such payments, especially when large numbers of distributed renewable generation are considered. Questions along those lines are seen as an interesting topic for future research.

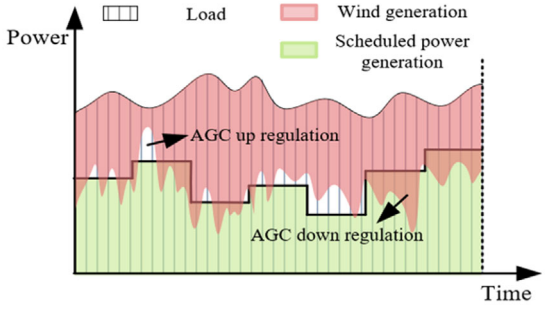

FIGURE 2 Power balance in wind embedded grid

System-wide power imbalances are compensated in real-time by AGC units. While different system operators use different methods to purchase secondary reserves, one common solution are hourly markets based on mileage payments. For example, according to [26], PJM clears the market by co-optimizing energy and regulation for each operating hour subject to regulation capacity constraints. Similarly, in China Southern Power Grid (CSG) market, the regulation market is also cleared each hour [27]. In this work, we assume that all AGC units bid for their regulation capability hourly ahead, and the market clears the mileage price periodically based on specific information including bid-in prices and historical performance indices of individual AGC units.

The mileage payment quantitatively reflects the regulation engagement of AGC units. In a specific AGC cycle t, the mileage payment to AGC unit m can be obtained by

$$\gamma_m(t) = |D_m(t)| \cdot S \cdot K_m, \tag{1}$$

where $D_m(t)$ denotes the active power injection or withdrawal from regulation unit m when following the AGC dispatch signal at AGC cycle t, S is the market dependent mileage price, and the performance score K_{m} reflects the general performance of unit m when following the dispatch signals. $D_m(t)$ can be expressed as

$$D_m(t) = P_m^{reg}(t) - P_m^{reg}(t-1), \tag{2}$$

where $P_m^{reg}(t)$ and $P_m^{reg}(t-1)$ are power output from unit m at control cycle t and previous control cycle $t-1$ respectively.

System operators use different metrics and methods to assign a performance score K_{m} to each AGC unit [28]. Here, we assume that the performance score is determined based on the following three metrics: regulation rate, response delay, and the regulation precision (the reader is referred to the Appendix for further details). The AGC units respond to a dispatch signal to balance generation and demand in the power system. This power balance requirement is illustrated in Figure 2 and can be expressed as

$$P_{load}(t) - P_{wind}(t) = P_{schedule}(t) + \sum_{m=1}^{M} D_m(t), \tag{3}$$

where M is the number of AGC units.

Specifically, in Figure 2, the pink area represents the wind generation; the green area represents the scheduled power generation by dispatchable sources. However, the sum of the pink and the green area are generally not equal to the demand. Specifically, upward AGC regulation is required if the sum of scheduled power generation and wind power generation is smaller than the demand and downward AGC regulation is required when the sum of wind power generation and scheduled power generation is larger than the load.

Due to the uncertain and intermittent characteristics of wind turbines would result in low performance scores if they were used as a conventional AGC units. In other words, in a performance-based regulation market wind farms would likely not be selected to contribute to AGC and provide secondary reserves. Nonetheless, WFs can be controlled to contributed to system-wide balancing needs, e.g., by down regulation and exploiting the energy stored in the wind turbine rotor. Finally, depending on the overall generation mix, a system operator may need to impose requirements for system balancing on the wind farms. For example, in a future system with large share of wind power penetration, the regulation capacity of the remaining conventional AGC units may not be sufficient to balance the system on the time scales of AGC. In this case WFs may be designated as balancing responsible.

2.2 | Principle of wind power regulation

For an individual WT, the mechanical power extracted from the wind is defined as

$$P_m = \frac{\rho}{2}\pi R^2 v^3 C_p(\lambda, \beta) \tag{4}$$

where ρ is the density of air, R is the rotor blade radius, v is the wind speed, λ is the tip speed ratio, and β is the pitch angle. Moreover, the power coefficient $C_p(\lambda, \beta)$ models the non-linear relationship between the pitch angle and tip speed ratio

$$\lambda = \frac{\omega R}{v} \tag{5}$$

where ω is rotor speed.

It should be noted that online optimal control of WTs is a challenging problem because the C_p is a highly non-linear function of the tip speed ratio and the blade pitch angle. To address this issue, an intelligent learning-based strategy is proposed in Ref. [29]. For computational purposes, the power coefficient can be approximated through the fourth order polynomial

$$C_p(\beta, \lambda) = [c_{11}\beta^2 + c_{12}\beta + c_{13}]\lambda^2 + [c_{21}\beta^2 + c_{22}\beta + c_{23}]\lambda + [c_{31}\beta^2 + c_{32}\beta + c_{33}] \tag{6}$$

obtained using polynomial regression. The resulting parameters for Equation (6) and approximation error are given in Table A1 and Table A2 in the Appendix. We emphasize that the approximation error is small, and the approximation Equation (6) can be directly used for the purpose of real-time control. It should be noted that the tip speed ratio depends on the rotor speed, and that the rotor speed and the blade pitch angle are both control variables. Because the tip speed ratio and blade pitch angle are multiplied in Equation (6) the mechanical power Equation (4) is a non-convex function of the rotor speed and blade pitch angle.

Next, we consider the active power balance. For an individual WT, the KE stored in its rotating mass can be expressed as

$$E(t) = \frac{1}{2}J\omega^2(t), \tag{7}$$

where J denotes the combined wind rotor and generator inertia. Moreover, the imbalance between the captured mechanical power and the electric power delivered to system will lead to WT rotor speed variation. This process is modelled by the differential equation

$$P_m(t) - P_e(t) = P_k(t) = \frac{dE(t)}{dt} = J\omega(t)\frac{d\omega(t)}{dt}, \tag{8}$$

where P_e is the WT electric power output.

It should be noted that the WT control variables in our model are updated at each AGC cycle (i.e. 4 s). To this end, the differential Equation (8) is discretised to obtain

$$P_e(t) = P_m(t) - J\omega(t)\frac{\omega(t) - \omega(t-1)}{\Delta t}, \tag{9}$$

where Δt is the AGC cycle.

It follows from Equation (9), that the WT power output can be regulated by adjusting the rotor speed within its operational constraints. It should be noted that WTs might stall if too much KE is extracted. To avoid this problem, the electric power output of an individual WT should be limited to

$$P_e(t) \le P_{mmp}(t) + P_{k\max}^{disc}(t), \tag{10}$$

where P_{mmp} is the maximum mechanical power that the WT captures from wind given by

$$P_{mmp} = \begin{cases} \frac{1}{2}\rho A C_{p\max} v^3, v \le v_{rated} \\ P_{nom}, v > v_{rated} \end{cases}, \tag{11}$$

$C_{p\max}$ denotes the maximum power coefficient, and P_{nom} denotes the WT nominal power. Equation (11) highlights the two standard operating regimes of WTs. When the wind speed is lower than the rated value, WT typically operates in MPPT mode (i.e. at zero pitch angle and optimal rotor speed). In contrast, above the rated wind speeds, the pitch angle is increased to capture the (constant) nominal power and keep the rotor speed at the (constant) nominal speed.

We emphasize that our control approach will not use MPPT control, but leverage the ability to control the power injection

within the limits set by Equation (10), where $P^{disc}_{k\max}$ denotes the maximum electric power released from KE discharging. As reported in [30], a WT operating at a rotor speed below the maximum power point (MPP) rotor speed may pose less small signal stability margin. To avoid this problem, we define the maximum discharge power $P^{disc}_{k\max}$

$$P^{disc}_{k\max}(t) = \frac{E(t-1) - E(t)}{\Delta t} = \frac{J(\omega^2(t) - \omega^2_{mmp}(t))}{2\Delta t}, \quad (12)$$

where ω_{mmp} is the rotor speed at MPP which can be calculated using Equation (11) and the wind speed, and limit the KE discharge according to Equations (10) and (12) to ensure that the WT returns to the MPP after releasing the stored KE.

In addition to adjusting the rotor speed, the blade pitch angle can be used to regulate the electric power delivered to the grid. However, when increasing the pitch angle to reduce power generation, excess energy is discarded. In contrast, rotor speed control can be used to store excess power in the form of KE. Because our objective is to minimize the mileage cost without significantly reducing energy yield, the proposed controller will prioritize rotor speed control and only use blade pitch angle control when needed.

2.3 | Optimal wind power regulation scheme

As discussed in Section 2.1, WTs can be controlled as semi-dispatchable units for the purpose of power balancing. However, there is an inherent trade-off between wind energy yield maximization and balancing cost minimization. To concurrently consider these two objectives, we formulate a joint optimization problem.

According to Equation (9), the output power of WTs is coupled across different time steps. Therefore, to optimize control performance, we propose to use the following receding horizon optimization problem that is solved by the WF operator to obtain dispatch commands for the WTs:

$$\min_{\omega_b(t),\beta_b(t),P^{reg\_up}_m(t),P^{reg\_down}_m(t)\in\mathbb{R}^+} -\alpha \sum_{t=t_0}^{t_T}\sum_{b=1}^{B} P_{e,b}(t)/P_{wfnom} + (1-\alpha)\sum_{t=t_0}^{t_T}\sum_{m=1}^{M}\left|(D^{up}_m(t) + D^{down}_m(t))\right| SK_m/C_{mil\max} \quad (13)$$

$$\text{s.t. } \omega_{\min} \le \omega_b(t) \le \omega_{\max} \quad (14)$$

$$\beta_{\min} \le \beta_b(t) \le \beta_{\max} \quad (15)$$

$$P_{e,b}(t) \le P_{mpp,b}(t) + \max\left\{0, P^{disc}_{k\max,b}(t)\right\} \quad (16)$$

$$P^b_e(t) \le 1.2P_{nom} \quad (17)$$

$$D^{up}_m(t) = P^{reg\_up}_m(t) - P^{reg\_up}_m(t-1) \quad (18)$$

$$D^{down}_m(t) = P^{reg\_down}_m(t-1) - P^{reg\_down}_m(t) \quad (19)$$

$$0 \le P^{reg\_up}_m(t) \le P^{reg\_cap}_m \quad (20)$$

$$0 \le P^{reg\_down}_m(t) \le P^{reg\_cap}_m \quad (21)$$

$$P_{load}(t) - P_{wind}(t) = P_{schedule}(t) + \sum_{m=1}^{M}(D^{up}_m(t) - D^{down}_m(t)) \quad (22)$$

where Equations (4), (5), and (9) are used to predict the rotor speed for each time step.

Objective: The first term in Equation (13) aims to maximize the total wind power production. The second term aims to minimize the system-wide mileage payment within the time horizon t_T that will be partially allocated to the WF. In Equation (13), M is the number of AGC units, B is the number of WTs, $P_{e,b}(t)$ is the power output of individual WTs, and P_{wfnom} as well as $C_{mil\max}$ are the nominal power of the WF and the maximum mileage cost, respectively. As mentioned before, in this work, we assume that the WF should be partially balancing responsible by consider the mileage payment as a metric for system-wide power imbalance and wind power regulation. To this end, the weighting factor $\alpha \in [0, 1]$ in Equation (13) can be used to give more or less weight to balancing cost.

WT constraints: To ensure reliable operation of individual WTs, the control action is subject to certain practical constraints in Equations (14)–(17). Specifically, the power injection of individual WTs is subject to converter power limits (assumed to be 1.2 p.u.). Moreover, to avoid stalling the WT, the power output of individual WTs is constrained by Equation (16). Finally, the rotor speed and pitch angle variations throughout the dynamic operation are subject to the constraints in Equations (14), (15).

System constraints: The AGC units that participate in the regulation market are subject to operational constraints in Equations (18)–(21), where $D^{up}_m(t)$ ($D^{down}_m(t)$) denote up- (down-) regulation mileage and $P^{reg\_up}_m(t)$ ($P^{reg\_down}_m$) denote up- (down-) regulation power of AGC unit m. Moreover, $P^{reg\_cap}_m$ denotes the regulation capacity of AGC unit m. Finally, the system should satisfy power balancing constraint Equation (22) in each AGC interval.

The wind-farm level optimization problem in Equations (13)–(22) does not include a detailed model of the wind turbine's inner control loops, which is often not exactly known to the wind-farm operator. Instead, we separate the control problem into wind-farm level optimization and a wind-turbine control that is compatible with standard wind farm control architectures and discussed in the next section.

For the case studies in Section 4, the receding horizon optimization problem will be solved using the Interior Point OPTimizer (IPOPT). Even though the first term of Equation (13)

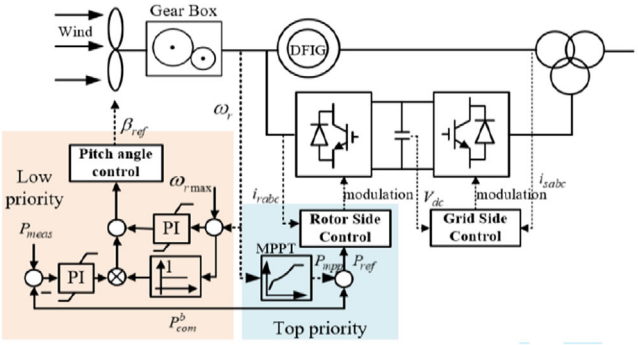

FIGURE 3 Proposed prioritized control for wind power regulation

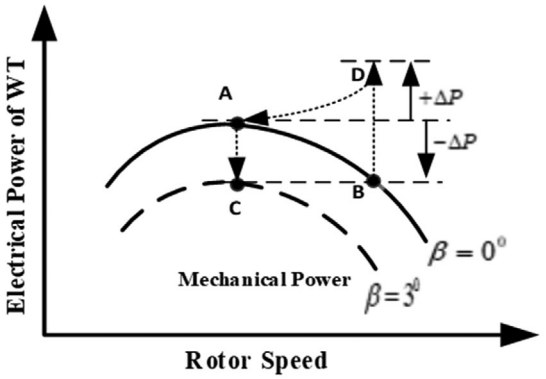

FIGURE 4 Control dynamics of rotor speed control and pitch angle control

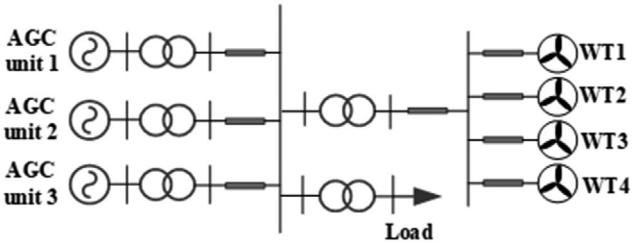

FIGURE 5 Configuration of the test system

is non-convex, the problem (i) can be solved efficiently within one AGC control cycle; (ii) results in effective wind power regulation; and iii) we observe no practical constraint violations.

3 | PRIORITIZED CONTROL OF WIND TURBINES FOR POWER REGULATION

Typically, WTs operate in MPPT control mode and are not required to share balancing responsibility. In this setting, the active power reference is generated via a MPPT curve and tracked by the rotor side controller (see Figure 3,). Moreover, if the rotor speed is larger than the maximum value, a PI controller is used to control to the blade pitch angle and limit the rotor speed to its maximum value. In contrast, we propose to bypass the MPPT control and utilize both rotor speed control and pitch angle control to track a wind power reference obtained from the receding horizon optimization Equations (13)–(22). As discussed in Section 2.2, rotor speed control can achieve higher efficiency a by leveraging kinetic energy storage. Moreover, the control objective formulated in Section 2.3, is to minimize the mileage cost without significantly reducing energy yield. This amounts to storing as much excess energy as possible as KE to i) achieve high energy harvesting efficiency and ii) create a sufficient "energy buffer" that enables the WT to track the dispatch commands. Hence, the proposed WT control prioritizes control strategy is designed, which is consistent with our optimization objective. As shown in Figure 3, the optimized active power reference is sent to the rotor side controller and blade pitch angle controller. Once the rotor speed is accelerated to its upper limit, the deviation between the measured active power output and the dispatch command will be sent to a PI controller to generate a pitch angle reference to force the WT to follow the reference.

Overall, as shown in Figure 1, the optimization module and WT control module are mutually influenced and closely coupled. The proposed WT cascade control has the following merits:

- energy harvesting efficiency can be increased by utilizing the rotor to store/release extra energy,
- WT system wear can be reduced by only using pitching control for power curtailment with low priority.

3.1 | Rotor speed and pitch angle control

The process supplementing wind power generation with kinetic energy is illustrated in Figure 4. Considering a WT that initially operates at the maximum power point (i.e. A), the operating point can be shifted to B to allow tracking the dispatch command. If the dispatch command is greater than the WT power at A, the WT can be controlled to shift to D by releasing the stored KE. Considering the fast response of the power electronic converters, the power output can be rapidly regulated according to the new reference. Moreover, starting from A, the WT can shift to C by increasing the pitch angle if the introduced power command is less than the WT power output. In contrast to rotor speed control, pure pitch control cannot leverage the KE storage capability and thus cannot provide overloading support.

4 | CASE STUDIES

4.1 | Experimental setup

(1) Test system. To demonstrate the effectiveness of the proposed WF power regulation scheme, the system shown in Figure 5 is used. It consists of 3 AGC units, a wind farm with 4 identical 5-MW DFIG wind turbines [31], and a time varying electrical load. Specifically, the WT model includes the aerodynamics, shaft dynamics, induction generator, pitch servo mechanism, and the controlled back-to-back converter. The parameters of the AGC units are specified in Table 1 and, together

TABLE 1 AGC units settings

AGC unit no.	Regulation capacity (MW)	Regulation rate	Response delay	Regulation precision
1	4	0.25	0.9833	0.5333
2	6	1.6667	0.8801	0.7870
3	8	1.0833	0.9227	0.6433

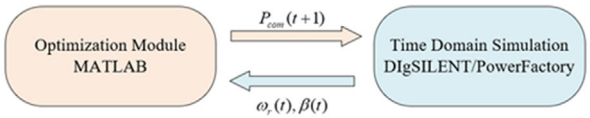

FIGURE 6 MATLAB-DIgSILENT joint simulation platform

with a mileage price of 1.1 $/MW, reflect typical parameter values that serve as approximation of the overall mileage payments and AGC action.

In the remainder we use wind speed data from [32] to evaluate multiple control strategies over a 15-min horizon. Without loss of generality, it is assumed that $P_{load} - P_{schedule} = P_{MPPT}^{3\,\min}$, where $P_{MPPT}^{3\,\min}$ denotes the 3-min averaged generation profile of wind power under MPPT control. The prediction horizon for the optimization is set as 5 AGC time slots (i.e. 20 s).

(2) Joint simulation platform. To verify the effectiveness of the proposed WF regulation scheme, a simulation platform is required that is both capable of handling receding horizon optimization as well as time-domain simulation of the test systems with multiple WTs, AGC units, and their control algorithms. To this end, we are combining MATLAB and DIgSILENT/PowerFactory as shown in Figure 6. DIgSILENT is used for detailed modelling of wind turbines and perform the time-domain simulation of the overall system. Moreover, for this validation study an interface facilitating bidirectional data exchange between MATLAB and DIgSILENT has been developed. Within each control cycle, MATLAB receives the current WT state (i.e. ω_{t0}, β_{t0}), solves the receding horizon optimization problem using IPOPT, and sends the dispatch commands to DIgSILENT.

The optimization module is run in MATLAB every 4 s, i.e. for every AGC cycle. Table 2 shows the average computation time and hardware used for this numerical experiment.

TABLE 2 Computational efficiency

Computation platform	Dell precision tower workstation
CPU	E5-2650 v4@2.20 GHz, 2 processors
Solver	IPOPT (interior-point method), OPTI Toolbox in MATLAB
Computation time	0.2732 s (averaged by 10,000 individual runs)

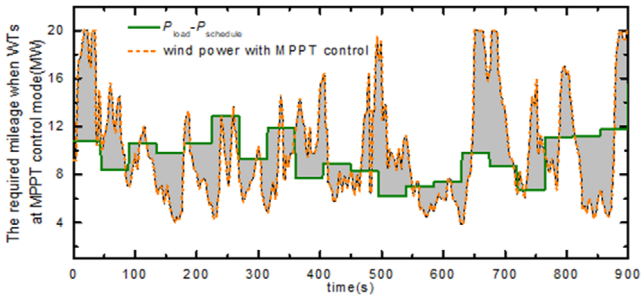

FIGURE 7 The required regulation mileage when WTs operate at the MPPT control mode

4.2 | Wind power regulation performance comparisons

According to Equation (3), the regulation mileage can be calculated as $P_{load} - P_{schedule} - P_{wind}$. In our case study, when WTs operate at MPPT control mode, the required mileage for system balance is given by the grey area in Figure 7. Specifically, downward regulation is needed when the wind power generation is above the green line. On the other hand, upward regulation is needed when the wind power generation is below the green line.

Next, we compare three dispatch command generation methods in our simulations: (i) our proposed scheme, i.e. the system-perceived method, (ii) the Moving Average (MA) method, and (iii) the Low-pass Filter (LPF) method.

We evaluate the wind power regulation performance of different methods according to the following metrics.

Wind energy yield ψ(kWh): It is formulated as

$$\sum_{t=t_0}^{t_T} \sum_{b=1}^{B} P_{e,b}(t) \Delta t. \tag{23}$$

Total mileage payment ζ ($): It is formulated as

$$\sum_{t=t_0}^{t_T} \sum_{m=1}^{M} \left| (D_m^{up}(t) + D_m^{down}(t)) \right| SK_m. \tag{24}$$

Power reference tracking error δ: To quantitatively evaluate the reference tracking performance of the WT controls for each dispatch strategy, we define the tracking error:

$$\delta = \sqrt{1/N \sum_{i=1}^{N} (P_{meas} - P_{com})^2} \tag{25}$$

where P_{meas} denotes the measured actual power output from the WF and P_{com} denotes the power reference for the WF.

The main parameters and resulting performance metrics are summarized in Table 3 and shown in Figures 8–10. For the MA method, n is the pre-defined averaging window size. In the LPF method, T_{LPF} is the time constant used to specify the cut-off

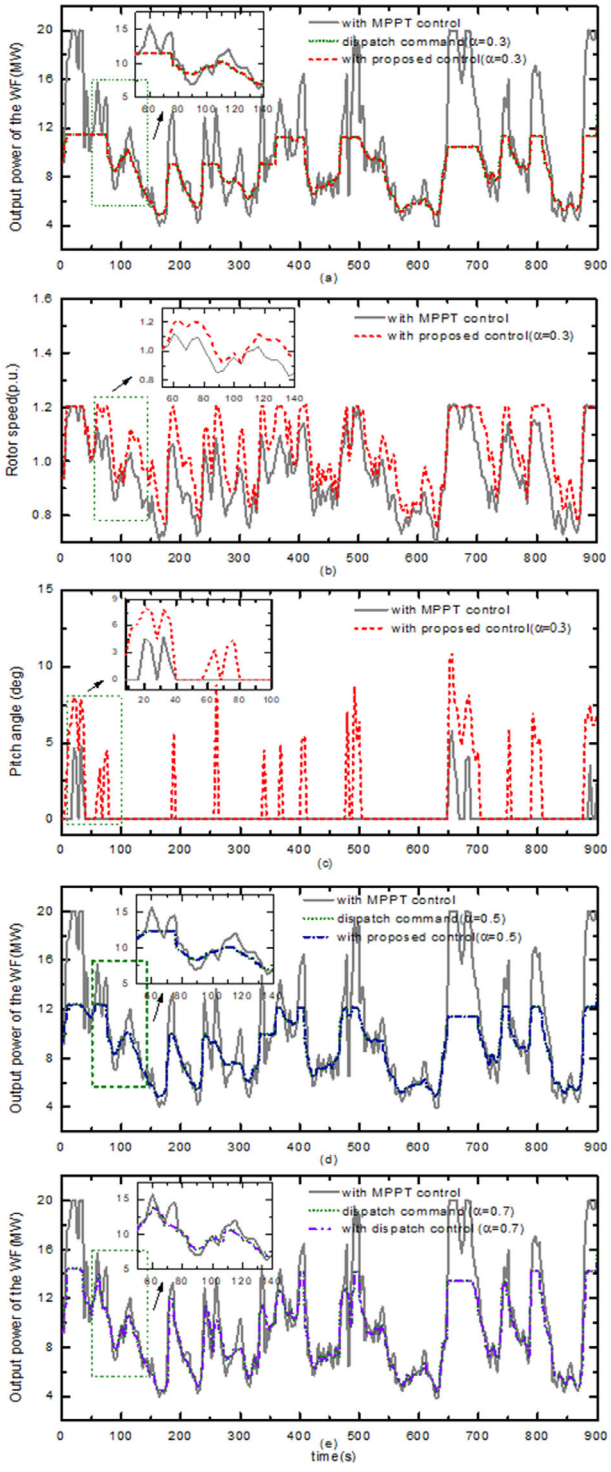

FIGURE 8 Simulation results using the proposed control framework. (a) Total output power of the WF ($\alpha = 0.3$); (b) rotor speed; (c) pitch angle; (d) total output power of the WF ($\alpha = 0.5$); (e) total output power of the WF ($\alpha = 0.7$)

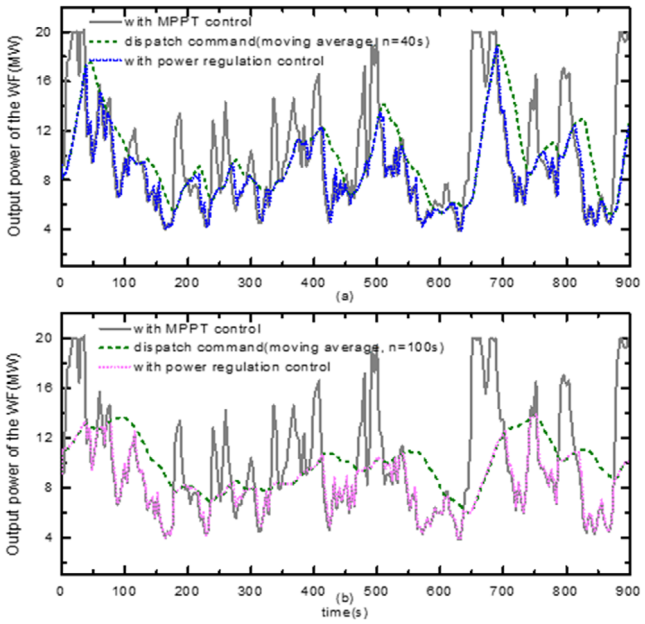

FIGURE 9 Simulation results of MA method. (a) Total output power of the WF ($n = 40$ s); (b) total output power of the WF ($n = 100$ s)

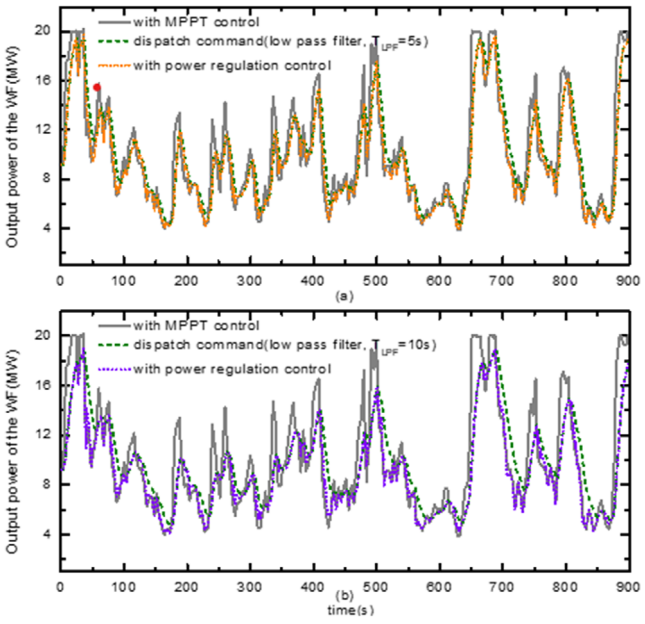

FIGURE 10 Simulation results of LPF method. (a) Total output power of the WF (TLPF = 5 s); (b) total output power of the WF (TLPF = 10 s)

frequency of the LPF. For all methods, the prioritized WT control strategy proposed in Section 3 is used to track the dispatch command.

In our proposed control paradigm, the WT dispatch is obtained through a receding horizon optimization that considers the trade-off between maximizing wind energy harvesting and minimizing mileage cost. The results in Table 3 illustrate that the total captured wind energy decreases as α is decreased. Curtailment of wind energy occurs because downward AGC regulation is required in some situation, as shown in the grey area above the green line in Figure 7. It should be noted that the wind energy curtailment is not arbitrary but minimizes power imbalances and mileage payments. Moreover, as expected, the mileage payments decrease as α is decreased. In comparison with the receding horizon control with $\alpha = 0.3$, the MA method

TABLE 3 Comparative simulation results

	$\alpha = 0.3$	$\alpha = 0.5$	$\alpha = 0.7$
System-perceived method	$\psi = 2154.73$ $\zeta = 38.68$ $\delta = 0.155$	$\psi = 2213.87$ $\zeta = 64.50$ $\delta = 0.179$	$\psi = 2282.56$ $\zeta = 86.28$ $\delta = 0.248$
	$n = 40$s	$n = 100$s	
MA	$\psi = 2140.64$ $\zeta = 55.48$ $\delta = 2.106$	$\psi = 2104.04$ $\zeta = 44.95$ $\delta = 2.521$	
	$T_{\text{LPF}} = 5$s	$T_{\text{LPF}} = 10$s	
LPF	$\psi = 2383.47$ $\zeta = 119.90$ $\delta = 0.779$	$\psi = 2304.59$ $\zeta = 98.63$ $\delta = 1.288$	

TABLE 4 Simulation results for different forecast accuracies (15 min of simulated wind speed series, $a = 0.7$)

Forecasting accuracy	Mileage payment $
Case 1: $\sigma_1 = 0.96$, $\sigma_2 = 0.945$, $\sigma_3 = 0.925$, $\sigma_4 = 0.90$, $\sigma_5 = 0.87$	87.45
Case 2: $\sigma_1 = 0.94$, $\sigma_2 = 0.925$, $\sigma_3 = 0.905$, $\sigma_4 = 0.88$, $\sigma_5 = 0.85$	89.80
Case 3: $\sigma_1 = 0.92$, $\sigma_2 = 0.905$, $\sigma_3 = 0.885$, $\sigma_4 = 0.86$, $\sigma_5 = 0.83$	91.16

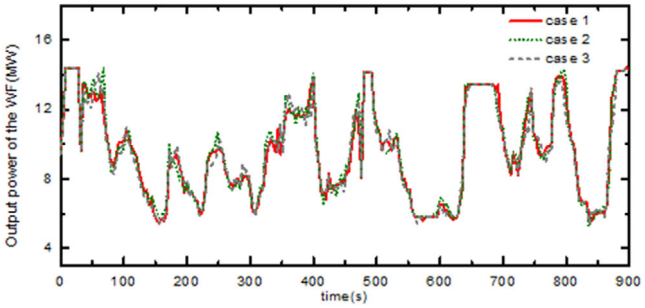

FIGURE 11 Wind farm generation profiles with different look-ahead forecasting accuracy

results in both less wind energy harvesting and higher mileage payments. Similarly, the LPF method results in significantly larger mileage payments than the proposed method but only achieves a slightly higher yield than the proposed method for $\alpha = 0.7$. In other words, from a system-level perspective, the proposed method outperforms ad-hoc smoothing algorithms by adjusting the WF power output in real-time to respond to the system balancing needs and balancing cost. As indicated in Table 3, the proposed framework has the smallest tracking error, i.e. the optimized dispatch commands were best tracked by the prioritized WT control.

Figures 8(a,d,e) and 9 show that the proposed control is effective in regulating output wind power. To track the WF power reference, the degrees of freedom of the WTs are adequately utilized through the proposed control strategy. As shown in Figure 8(b,c), when curtailment is required, a portion of the curtailed power is converted to KE by accelerating the rotor. Once the rotor speed reaches its maximum, the blade pitch angle control is activated to limit the power production. In contrast, the KE stored in the WT rotor is released back to system by decelerating the rotor when overloading is needed. Due to the constraint Equation (16), excessive rotor speed decelerations are avoided, and stable operation of the WTs is preserved.

4.3 | Influence of wind speed forecasting accuracy

To illustrate the impact of wind forecast uncertainty on the receding horizon optimization control Equations (13)–(22), different levels of forecasting accuracy are considered. Simulation results are reported in Table 4 and Figure 11 and we use σ_i to denote the wind speed forecasting accuracy in the i-th look-ahead time slot. Table 4 shows a slight increase in the mileage payments as the forecast error increases, i.e. forecast errors have an impact on the system-wide balancing cost. Nonetheless, we expect wind forecasts to be sufficiently accurate over the relatively short prediction horizon used in the proposed control. Moreover, compared to the MA and LPF methods (as indicated in Table 3), the proposed control strategy still effectively reduces the balancing cost despite the forecast errors. This observation can be explained by the receding horizon implementation of the proposed optimization-based control that recomputes the dispatch command at every AGC interval in closed-loop with the system and thereby accounts for deviations from the forecast.

5 | CONCLUSION

We propose a novel wind power regulation scheme that jointly accounts for system balancing cost reduction and wind power production maximization. In contrast to conventional methods that smooth the wind power production without considering the system-wide power imbalance, in this work, the wind power regulation explicitly accounts for the system balancing needs. Moreover, WT constraints are considered in the problem formulation to ensure that their real-time regulation capabilities are accurately reflected in the receding horizon control. Case studies and high-fidelity time-domain simulations are used to compare the proposed WF control scheme to standard power smoothing methods and verify the effectiveness and potential of the proposed approach. The influence of wind forecasting errors is also discussed in this work. Simulation results demonstrate that the proposed control exhibits satisfactory performance if the forecasting accuracy is sufficient. Specifically, the impact of forecast errors is mitigated because the receding control recomputes the dispatch command at every control cycle and thereby accounts for deviations from the forecast.

ACKNOWLEDGMENTS

This work was partially supported by Natural Science Foundation of China, 72071100; Guangdong Basic and Applied Basic Research Fund 2019A1515111173; Young Talent

Program of Guangdong, 2018KQNCX223; and High-level University Fund, G02236002.

ORCID

Youwei Jia https://orcid.org/0000-0003-3071-5552

REFERENCES

1. Xiong, L., et al.: Modeling and stability issues of voltage-source converter dominated power systems: A review. CSEE J. Power Energy Syst. (2020)
2. Joos, M., Staffell, I.: Short-term integration costs of variable renewable energy: Wind curtailment and balancing in Britain and Germany. Renewable Sustainable Energy Rev. 86, 45–65 (2018)
3. 2010 Wholesale Power and Transmission Rate Adjustment Proceeding (BPA-10). https://www.bpa.gov/Finance/RateCases/InactiveRateCases/Pages/WP-10-Rate-Case.aspx (2010). Accessed 2010.
4. "Tariff for maintaining and restoring the individual balance of access responsible parties. http://www.elia.be/~/media/files/Elia/Products-andservices/Balancing/Imbalance_2012-2015_EN.pdf. Accessed 2015.
5. Introduction to Charging: Which Parties Pay Which Charges. https://www.nationalgrid.com/sites/default/files/documents/44939-TNUoS%2C%20BSUoS%20and%20Connection%20Charging%20Information.pdf (2015). Accessed 2015.
6. Federal Energy Regulatory Commission. Order No. 755. Frequency Regulation Compensation in the Organized Wholesale Power Market (2011)
7. Papalexopoulos, A.D., Andrianesis, P.E.: Performance-based pricing of frequency regulation in electricity markets. IEEE Trans. Power Syst. 29, 441–449 (2014)
8. He, G., et al.: Poolla, K. Cooperation of wind power and battery storage to provide frequency regulation in power markets. IEEE Trans. Power Syst. 32, 3559–3568 (2016)
9. Hellmers, A., et al.: Operational strategies for a portfolio of wind farms and CHP plants in a two-price balancing market. IEEE Trans. Power Syst. 31, 2182–2191 (2015)
10. Jiang, Q., Wang, H.: Two-time-scale coordination control for a battery energy storage system to mitigate wind power fluctuations. IEEE Trans. Energy Convers. 28, 52–61 (2013)
11. Guo, T., et al.: A dynamic wavelet-based robust wind power smoothing approach using hybrid energy storage system. Int. J. Electr. Power Energy Syst. 116, 105579 (2020)
12. Guo, T., et al.: Two-stage optimal MPC for hybrid energy storage operation to enable smooth wind power integration. IET Renewable Power Gener. 14, 2477–2486 (2020)
13. Zhao, X., Yan, Z., Zhang, X.-P.: A wind-wave farm system with self-energy storage and smoothed power output. IEEE Access 4, 8634–8642 (2016)
14. Lyu, X., et al.: Coordinated control strategies of PMSG-based wind turbine for smoothing power fluctuations. IEEE Trans. Power Syst. 34, 391–401 (2018)
15. Zhou, Y., Yan, Z., Li, N.: A novel state of charge feedback strategy in wind power smoothing based on short-term forecast and scenario analysis. IEEE Trans. Sustainable Energy 8, 870–879 (2017)
16. Khalid, M., Savkin, A.: Minimization and control of battery energy storage for wind power smoothing: Aggregated, distributed and semi-distributed storage. Renewable Energy 64, 105–112 (2014)
17. Lyu, X., et al.: Mileage-responsive wind power smoothing. IEEE Trans. Ind. Electron. 67, 5209–5212 (2020)
18. Qais, M.H., Hasanien, H.M., Alghuwainem, S.: Output power smoothing of wind power plants using self-tuned controlled SMES units. Electr. Power Syst. Res. 178, 106056 (2020)
19. Koiwa, K., et al.: One-sample optimal output smoothing method for wind farm with energy storage system. IET Renewable Power Gener. 15, 653–663 (2021)
20. de Carvalho, W.C., et al.: Fuzzy-based approach for power smoothing of a full-converter wind turbine generator using a supercapacitor energy storage. Electr. Power Syst. Res. 184, 106287 (2020)
21. Thapa, K.B., Jayasawal, K.: Pitch control scheme for rapid active power control of a PMSG-based wind power plant. IEEE Trans. Ind. Appl. 56, 6756–6766 (2020)
22. Zhao, X.; Lin, Z.; Fu, B.; Gong, S.: Research on frequency control method for micro-grid with a hybrid approach of FFR-OPPT and pitch angle of wind turbine. Int. J. Electr. Power Energy Syst. 127, 106670 (2021)
23. Yoo, J.I., et al.: Power smoothing of a variable-speed wind turbine generator based on a two-valued control gain. IEEE Trans. Sustainable Energy 11, 2765–2774 (2020)
24. Dong, Z., et al.: Fully-distributed deloading operation of DFIG-based wind farm for load sharing. IEEE Trans. Sustainable Energy 12, 430–440 (2020)
25. Ravanji, M.H., Cañizares, C.A., Parniani, M.: Modeling and control of variable speed wind turbine generators for frequency regulation. IEEE Trans. Sustainable Energy 11, 916–927 (2019)
26. PJM Manual 11: Energy & Ancillary Services Market Operations. https://www.pjm.com/-/media/documents/manuals/m11.ashx (2021). Accessed 2021.
27. Detalied Ruls for Guangdong Frequency Regulation Auxiliary Service Market. http://nfj.nea.gov.cn/adminContent/initViewContent.do?pk=402881e56579be6301658d99ac57001f (2018). Accessed 2018.
28. Ko, K.S., Han, S., Sung, D.K.: Performance-based settlement of frequency regulation for electric vehicle aggregators. IEEE Trans. Smart Grid 9, 866–875 (2018)
29. Lyu, X., et al.: System-oriented power regulation scheme for wind farms: The quest for uncertainty management. IEEE Trans. Power Syst. (2021)
30. Janssens, N.A., Lambin, G., Bragard, N.: Active power control strategies of DFIG wind turbines. In: Proceedings of Conference on Active Power Control Strategies of DFIG Wind Turbines. Lausanne, Switzerland, pp. 516–521 (2007)
31. Jonkman, J., et al.: Definition of a 5-MW reference wind turbine for offshore system development. *Technical Report No NREL/TP-500-38060*. National Renewable Energy Laboratory, Golden, CO (2009)
32. Database of Wind Characteristics. http://www.winddata.com/. Accessed 2020.

How to cite this article: Lyu, X., et al.: Optimal power regulation for wind integration in the balancing market environment. IET Renew. Power Gener. 2021;15: 3601–3611. https://doi.org/10.1049/rpg2.12248.

APPENDICES

A1 Performance score calculation

Regulation rate score: This score quantifies the regulation rate of the resource in response to the dispatch signal, which is a per-unit value calculated as

$$k_m^{rate} = P_m^{rate} / P_{avg}^{rate} \tag{A1}$$

where P_m^{rate} is the maximum ramp rate of unit m, P_m^{rate} is the average ramp rate of the control area.

TABLE A1 Fitting parameters of C_p

Model	$C_p(\beta_t, \lambda_t) = [c_{11}\beta_t{}^2 + c_{12}\beta_t + c_{13}]\lambda_t^2 + [c_{21}\beta_t{}^2 + c_{22}\beta_t + c_{23}]\lambda_t + [c_{31}\beta_t{}^2 + c_{32}\beta_t + c_{33}]$				
c_{11}	-1.9543×10^{-4}	c_{21}	1×10^{-3}	c_{31}	-1.5×10^{-3}
c_{12}	1×10^{-3}	c_{22}	-1.01×10^{-2}	c_{32}	2.06×10^{-2}
c_{13}	-9.4×10^{-3}	c_{23}	1.538×10^{-1}	c_{33}	-1.969×10^{-1}

TABLE A2 Approximation error

MAPE	0.1236
NRMSE	0.1112

Response delay score: This score quantifies the time delay between AGC signal and output change of regulation resource, which can be expressed as

$$k_m^{delay} = 1 - T_m^{delay} \Big/ 5\,\text{min} \tag{A2}$$

where T_m^{delay} is the response delay time of unit m.

Regulation precision score: This score measures the control performance of AGC units, which is expressed as

$$k_m^{precision} = 1 - \frac{1}{N}\sum_{i=1}^{N}\left|\frac{P_m^{disp} - P_m^{act}}{P_m^{avg}}\right| \tag{A3}$$

where P_m^{disp} is the AGC dispatch signal of unit m,P_m^{act} is the actual output of unit m,P_m^{avg} is the average absolute value of AGC dispatch signal of unit m during N control cycles.

The overall performance score can be calculated through a weighted sum of k_m^{rate},k_m^{delay} and $k_m^{precision}$, i.e.

$$K_m = a_1 k_m^{rate} + a_2 k_m^{delay} + a_3 k_m^{precision} \tag{A4}$$

where a_1, a_2, and a_3 represent non-negative weights and satisfy $a_1 + a_2 + a_3 = 1$. The weights are generally determined by the ISO based on the historical regulation performance of individual AGC units. In our study, we set "$a_1 = 0.5$, $a_2 = 0.25$, $a_3 = 0.25$" as an example, which can be flexibly changed in different operation scenarios.

A2 Polynomial regression of the power coefficient